

Coriolis coupling in the rotational bands of deformed odd-odd nuclei

A. K. Jain,* J. Kvasil,[†] and R. K. Sheline
Florida State University, Tallahassee, Florida 32306

R. W. Hoff

Lawrence Livermore National Laboratory, Livermore, California 94550

(Received 3 March 1989)

Evidence is presented for the existence of odd-even staggering in K^- rotational bands (with $K > 0$) of odd-odd nuclei in the rare-earth and actinide regions. Coriolis-coupling calculations have been carried out for rotational bands in ^{168}Tm , ^{176}Lu , ^{182}Ta , and ^{182}Re . With these calculations, we are able to reproduce the odd-even staggering observed in these nuclei. In particular, the unusually strong staggering observed in the $K=2^+$ and 4^- bands of ^{182}Re can be understood. Unusual features in the wave functions of some bands reflect the importance of couplings due to terms other than Coriolis in the Hamiltonian.

I. INTRODUCTION

It is now well recognized that the Coriolis force plays an important role in influencing the structure of deformed nuclei both at low and high spins. Although many Coriolis band-mixing calculations have been carried out in the past for rotational bands in odd-odd nuclei, these calculations have been limited in scope and have usually attempted to mix only two or three known bands. In fact, it has generally been thought¹ that odd-odd nuclei should have more exact rotational energy systematics because of the experimentally observed large moments of inertia and decreased pairing. However, recent high-spin data for the $K=2^+$ and 4^- bands in ^{182}Re exhibit a high degree of distortion.² This focused our attention on questions of the degree and the extent to which Coriolis distortion is present in rotational bands of odd-odd nuclei. An examination of the experimental data revealed that practically all $K^- \equiv |k_p - k_n|$ bands exhibit an odd-even staggering. In a preliminary report, we explained this odd-even shift for bands with $K > 0$ in terms of Coriolis coupling of rotational bands.³ In the present paper we report the detailed results of our calculations and show why the K^- bands exhibit greater staggering than do the K^+ bands. We show that the magnitude of the staggering is a function of the quasiparticle matrix elements of the Nilsson orbitals occupied by the unpaired nucleons. We also identify three basic mechanisms responsible for staggering and the cases where they might apply. We find clear evidence for the effects of second and higher orders of Coriolis coupling. An important aspect of the present work is that we try to do a complete Coriolis-coupling calculation, thus including both the known and the important unknown bands.

II. EMPIRICAL DATA ON ODD-EVEN STAGGERING

In Figs. 1 and 2 we summarize the empirical evidence for odd-even staggering in rotational bands of nuclei in the rare-earth and the actinide regions, respectively. In

these figures, we plot the ratio $\Delta E(I \rightarrow I-1)/2I$ vs $2I^2$ for all the $K^- = |k_p - k_n|$ bands where experimental data are available except for $K=0$ bands, which are known to be staggered as a consequence of the residual neutron-proton interaction. Although one expects linear behavior in such a plot if a rotational band behaves according to the usual $I(I+1)$ formula, all but two of the bands in Fig. 1 exhibit an odd-even staggering or perturbation in the sequence of effective values for the rotational parameter. It can be seen that the magnitude of the staggering is quite variable, ranging from strong fluctuations to only a minor effect. The effect is greatest in the case of one of the $K=1^+$ bands in ^{154}Eu , where the 1^+ level has been pushed above the 2^+ level. Certain other bands exhibit no detectable staggering, e.g., the $K=3^+$ band of ^{166}Ho and one of the $K=2^-$ bands in ^{182}Ta . We have not included in our discussion the strong odd-even effect observed in the highly aligned bands of many odd-odd nuclei and explicitly labeled as $(h_{11/2})_p(i_{13/2})_n$ mixed bands.⁴

In contrast, only one of the nine $K^+ = |k_p + k_n|$ bands in the rare-earth region for which data are available shows any odd-even staggering. The exception, a $K^+=5^-$ band in ^{158}Ho , behaves in a manner indicating that it might be an $(h_{11/2})_p(i_{13/2})_n$ mixed band similar to those observed in ^{160}Ho and ^{162}Ho . If this is the case, the odd-even staggering can be understood. In making this survey, we have excluded $K^+=1$ bands that arise from a coupling of a $k_p = \frac{1}{2}$ proton and a $k_n = \frac{1}{2}$ neutron. In this case, since the K^+ bands are directly coupled to $K^-=0$ bands, they obviously will show an odd-even effect.

Fewer rotational bands have been characterized in the odd-odd nuclei of the actinide region. The K^- bands are summarized in Fig. 2. Included in the figure are Gallagher-Moszkowski (G-M) doublets with $K^-=2^-$ and $K^+=3^-$ for ^{240}Am and ^{242}Am . We conclude that K^- bands in the actinide region are also likely to show odd-even staggering. As for the staggering observed in the K^+ bands, it can be shown to be the direct result of an odd-even shift present in the K^- bands under the spe-

cial situation where one of the odd particles occupies a $k = \frac{1}{2}$ state.

Thus, out of the 43 K^- band where staggering is observed, 25 are $K=1$ bands and the rest are $K=2, 3$, and 4 bands. The origin of the odd-even staggering in the $K=1$ bands can immediately be traced to direct Coriolis coupling with the Newby-shifted $K=0$ bands.⁵ Therefore, it seems likely that the staggering in the $K=2, 3$, and 4 bands is due to higher order Coriolis coupling with the $K=0$ bands. However, as we shall show, at least two additional mechanisms may be operative.

III. THE MODEL AND THE METHODOLOGY

A. The model

In our calculations, we have used a two-quasi-particle plus rotor model⁶ (TQPRM) for the description of the low-lying energy spectra of deformed odd-odd nuclei.

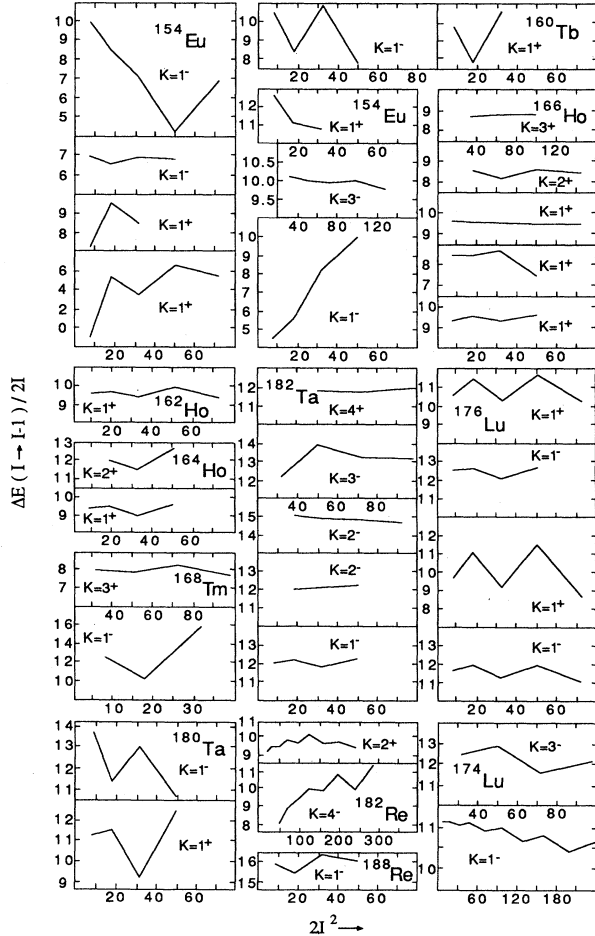


FIG. 1. Plots of $\Delta E(I \rightarrow I-1)/2I$ vs $2I^2$ for $K^- = |k_p - k_n|$ bands. Note that the scale is different in four plots of this figure. The data in this figure were taken from Ref. 17 and the following references: ¹⁵⁴Eu (Refs. 18, 19), ¹⁶⁰Tb (Ref. 20), ¹⁶²Ho (Ref. 21), ¹⁶⁴Ho (Refs. 20, 21), ¹⁶⁶Ho (Refs. 20, 22), ¹⁶⁸Tm (Refs. 23–25), ¹⁷⁴Lu (Refs. 26–29), ¹⁷⁶Lu (Refs. 30, 31), ¹⁸²Ta (Refs. 32, 33), ¹⁸²Re (Refs. 2, 34), and ¹⁸⁸Re (Refs. 35, 36).

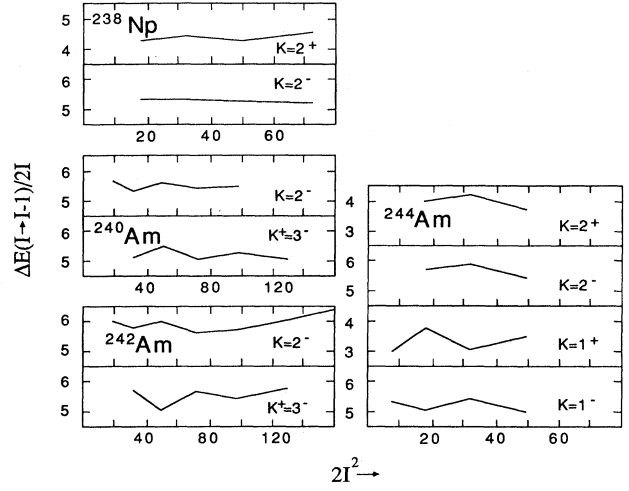


FIG. 2. Plots of $\Delta E(I \rightarrow I-1)/2I$ vs $2I^2$ for actinide nuclei. The data in this figure were taken from Ref. 17 and the following references: ²³⁸Np (Refs. 37, 38), ²⁴⁰Am (Ref. 39), ²⁴²Am (Ref. 39), and ²⁴⁴Am (Refs. 39, 40). Note that two of the plots correspond to K^+ bands, one each in ²⁴⁰Am and ²⁴²Am.

Since the model is well known, we discuss the necessary basic formulas for completeness. The total Hamiltonian of the system in the framework of the TQPRM is divided into two parts, the intrinsic and the rotational,

$$H = H_{\text{intr}} + H_{\text{rot}}. \quad (1)$$

The intrinsic part is given by a deformed, axially-symmetric average field H_{av} (such as in the Nilsson model); a short-range residual interaction H_{pair} (pairing); a long-range residual interaction H_{vib} , which is responsible for the vibrational degree of freedom; and a short-range neutron-proton interaction V_{np} , so that we have

$$H_{\text{intr}} = H_{\text{av}} + H_{\text{pair}} + H_{\text{vibr}} + V_{np}. \quad (2)$$

For an axially symmetric rotor with rotation axis perpendicular to the symmetry axis of the deformed average field, we can write

$$\begin{aligned} H_{\text{rot}} &= \frac{\hbar^2}{2\mathcal{J}} [(I_1 - j_1^2) + (I_2 - j_2^2)^2] \\ &= \frac{\hbar^2}{2\mathcal{J}} (I^2 - I_3^2) + H_{\text{Cor}} + H_{\text{ppc}} + H_{\text{irrot}}, \end{aligned} \quad (3)$$

where

$$H_{\text{Cor}} = -\frac{\hbar^2}{2\mathcal{J}} (I^+ j^- + I^- j^+), \quad (4a)$$

$$H_{\text{ppc}} = \frac{\hbar^2}{2\mathcal{J}} (j_p^+ j_n^- + j_p^- j_n^+), \quad (4b)$$

$$H_{\text{irrot}} = \frac{\hbar^2}{2\mathcal{J}} [(j_p^2 - j_{pz}^2) + (j_n^2 - j_{nz}^2)]. \quad (4c)$$

In Eq. (3), I_i and j_i ($i=1,2,3$) represent the components of total and intrinsic angular momentum, respectively. \mathcal{J} is the moment of inertia with respect to the rotation axis.

We assume that the even-even core is always in its vibrational ground state and, thus, neglect the long-range residual term H_{vibr} . The intrinsic angular momentum is given by the sum of the angular momentum of the odd-proton and the odd-neutron ($\mathbf{j} = \mathbf{j}_n + \mathbf{j}_p$). The operators $I^\pm = I_1 \pm iI_2$, $j^\pm = j_1 \pm ij_2$, $j_n^\pm = j_{n1} \pm ij_{n2}$, and $j_p^\pm = j_{p1} \pm ij_{p2}$ are the usual shifting operators.

The set of basis eigenvectors corresponds to the eigenfunctions of $H_{\text{av}} + H_{\text{pair}} + (\hbar^2/2\mathcal{J})(I^2 - I_3^2)$ and may be written in the form of the symmetrized product of Wigner functions D_{MK}^I and the intrinsic wave functions $|K\alpha\rangle$ as

$$|IMK\alpha\rangle = \left[\frac{2I+1}{16\pi^2(1+\delta_{K0})} \right]^{1/2} \times [D_{MK}^I |K\alpha\rangle + (-1)^{I+K} D_{M-K}^I R_i |K\alpha\rangle], \quad (5)$$

where the index α characterizes the configuration ($\alpha \equiv \rho_n \rho_p$) of the odd neutron and the odd proton such that $(H_{\text{av}} + H_{\text{pair}})|K\alpha\rangle = (\epsilon_{\rho_n} + \epsilon_{\rho_p})|K\alpha\rangle$ and where ϵ_{ρ_n} and ϵ_{ρ_p} are the quasiparticle neutron and proton energies of the respective quasiparticle states ρ_n and ρ_p . K is the projection of the intrinsic angular momentum onto the symmetry axis such that $j_3|K\alpha\rangle = K|K\alpha\rangle$ and coincides with the projection of total angular momentum in the case of an axially symmetric rotor. R_i is the operator representing rotation around the second intrinsic axis.

A rotational band can be built upon each intrinsic state $|K\alpha\rangle$. As a consequence of the symmetry of the average field, the projections Ω_n and Ω_p of the single quasiparticle angular momenta on the symmetry axis can couple in either parallel or antiparallel fashion. This gives rise to the Gallagher-Moszkowski doublets.

$$K^+ = (\Omega_p + \Omega_n) \text{ and } K^- = |\Omega_p - \Omega_n|. \quad (6)$$

The n - p residual interaction V_{np} splits the energy of this doublet—the so-called G-M splitting. We thus obtain two rotational bands for each two-quasi-particle configuration, the separation between the two bands being the G-M splitting energy. We use the symbol $\sigma = \pm$ to denote the two types of bands K^\pm . We can now write intrinsic wave functions $|K\alpha\sigma\rangle$ in terms of the quasiparticle wave function $|\rho\Omega\rangle$, as follows: for $K \neq 0$,

$$|K\alpha\sigma = +\rangle = |\rho_p \Omega_p\rangle |\rho_n \Omega_n\rangle, \quad (7a)$$

$$|K\alpha\sigma = -\rangle = |\rho_p \pm \Omega_p\rangle |\rho_n \mp \Omega_n\rangle, \quad (7b)$$

for $K=0$,

$$|K=0, \alpha\sigma = -\rangle = \frac{1}{\sqrt{2}} [|\rho_p \Omega\rangle |\rho_n - \Omega\rangle - (-1)^I |\rho_p - \Omega\rangle |\rho_n \Omega\rangle]. \quad (7c)$$

We also employ the usual approximation wherein the n - p residual interaction is treated in the first-order perturbation theory, thus neglecting all the nondiagonal matrix elements of V_{np} . We may point out that the effect of nondiagonal n - p residual interactions has recently been studied and may play a role in some cases.⁷ Even so, we can neglect these as they do not affect the outcome of our study, which mainly considers the effects of Coriolis coupling.

We may now write the matrix of the total Hamiltonian, Eq. (1), in an appropriate set of basis functions given by (5). We shall discuss the choice of the basis later on. We point out that this includes all of the two-quasi-particle configurations lying near the Fermi energy which are supposedly important in Coriolis mixing. To facilitate the writing of the Hamiltonian matrix, we further define the following quantities:

$$E_{\alpha+} = \epsilon_{\rho_n} + \epsilon_{\rho_p} + \langle \rho_p \Omega_p; \rho_n \Omega_n | V_{np} | \rho_p \Omega_p; \rho_n \Omega_n \rangle + \langle K\alpha+ | H_{\text{irrot}} | K\alpha+ \rangle, \quad (8a)$$

$$E_{\alpha-} = \epsilon_{\rho_n} + \epsilon_{\rho_p} + \langle \rho_p \Omega_p; \rho_n - \Omega_n | V_{np} | \rho_p - \Omega_p; \rho_n - \Omega_n \rangle + \langle K\alpha- | H_{\text{irrot}} | K\alpha- \rangle, \quad (8b)$$

$$C_\alpha \equiv \langle \rho_p \Omega_p; \rho_n - \Omega_n | V_{np} | \rho_p - \Omega_p; \rho_n \Omega_n \rangle. \quad (9)$$

Here $E_{\alpha\sigma}$ may be called band energies and C_α is the Newby term. We must point out that our definition of C_α differs from the quantity E_N of Ref. 6 by a phase factor of parity and by a sign from the quantity B of Ref. 8. The diagonal matrix elements of H_{irrot} have been absorbed in $E_{\alpha\sigma}$ which we will treat as a parameter. The term H_{irrot} will also have nondiagonal matrix elements with the selection rules $\Delta K = \Delta \Omega_p = \Delta \Omega_n = 0$ so that the intrinsic state of one of the particles must remain unchanged. In our calculations, we neglect these nondiagonal contributions.

In terms of these definitions the matrix elements of the total Hamiltonian can be expressed as

$$\langle IMK\alpha\sigma | H | IMK'\alpha'\sigma' \rangle$$

$$= \delta_{KK'} \delta_{\alpha\alpha'} \delta_{\sigma\sigma'} \left\{ E_{\alpha\sigma} + \frac{\hbar^2}{2\mathcal{J}} [I(I+1) - K^2] + \delta_{K0} \delta_{\sigma-} (-1)^{I+1} C_\alpha \right. \\ \left. + \delta_{K0} \delta_{\sigma-} (-1)^{I+1} \frac{\hbar^2}{2\mathcal{J}} \langle \rho_p \Omega | j_p^+ | \rho_p - \Omega \rangle \langle \rho_n \Omega | j_n^+ | \rho_n - \Omega \rangle \delta_{\Omega, 1/2} \right\} \\ + \delta_{KK'} \left\{ \delta_{\sigma+} \delta_{\sigma'} + \frac{\hbar^2}{2\mathcal{J}} [\langle \rho_p \Omega_p | j_p^+ | \rho_p' \Omega_p' \rangle \langle \rho_n \Omega_n | j_n^+ | \rho_n \Omega_n \rangle \delta_{\Omega_p, \Omega_p'+1} \delta_{\Omega_n, \Omega_n'+1} \right.$$

$$\begin{aligned}
& + \langle \rho'_p \Omega'_p | j_p^+ | \rho_p \Omega_p \rangle \langle \rho_n \Omega_n | j_n^+ | \rho'_n \Omega'_n \rangle \delta_{\Omega'_p, \Omega_p + 1} \delta_{\Omega_n, \Omega'_n + 1}] \\
& + \delta_{\sigma} + \delta_{\sigma'} - \frac{\hbar^2}{2\mathcal{J}} [\langle \rho'_p \Omega'_p | j_p^+ | \rho_p \Omega_p \rangle \langle \rho_n \Omega_n | j_n^+ | \rho'_n - \Omega'_n \rangle \delta_{\Omega'_p, \Omega_p + 1} \delta_{\Omega_n, 1/2} \delta_{\Omega'_n, 1/2} \\
& \quad + \langle \rho_p \Omega_p | j_p^+ | \rho'_p - \Omega'_p \rangle \langle \rho'_n \Omega'_n | j_n^+ | \rho_n \Omega_n \rangle \delta_{\Omega'_n, \Omega_n + 1} \delta_{\Omega_p, 1/2} \delta_{\Omega'_p, 1/2}] \\
& + \delta_{\sigma} - \delta_{\sigma'} + \frac{\hbar^2}{2\mathcal{J}} [\langle \rho_p \Omega_p | j_p^+ | \rho'_p \Omega'_p \rangle \langle \rho_n \Omega_n | j_n^+ | \rho'_n - \Omega'_n \rangle \delta_{\Omega_p, \Omega'_p + 1} \delta_{\Omega_n, 1/2} \delta_{\Omega'_n, 1/2} \\
& \quad + \langle \rho_p \Omega_p | j_p^+ | \rho'_p - \Omega'_p \rangle \langle \rho'_n \Omega'_n | j_n^+ | \rho_n \Omega_n \rangle \delta_{\Omega_n, \Omega'_n + 1} \delta_{\Omega_p, 1/2} \delta_{\Omega'_p, 1/2}] \\
& + \delta_{K0} \delta_{\sigma} - \delta_{\sigma'} - \frac{\hbar^2}{2\mathcal{J}} [- \langle \rho_p \Omega | j_p^+ | \rho'_p \Omega' \rangle \langle \rho_n \Omega | j_n^+ | \rho'_n \Omega' \rangle \delta_{\Omega, \Omega' + 1} \\
& \quad - \langle \rho'_p \Omega' | j_p^+ | \rho_p \Omega \rangle \langle \rho'_n \Omega' | j_n^+ | \rho_n \Omega \rangle \delta_{\Omega', \Omega + 1} \\
& \quad + (-1)^{I+1} \langle \rho_p \Omega | j_p^+ | \rho'_p - \Omega' \rangle \langle \rho_n \Omega | j_n^+ | \rho'_n - \Omega' \rangle \delta_{\Omega, 1/2} \delta_{\Omega', 1/2}] \Big\} \\
& + \delta_{K, K'-1} \left[- \frac{\hbar^2}{2\mathcal{J}} \right] \{ [(I+K')(I-K'+1)]^{1/2} \\
& \quad \times [\delta_{\sigma} + \delta_{\sigma'} + (\langle \rho'_p \Omega'_p | j_p^+ | \rho_p \Omega_p \rangle \delta_{\Omega'_p, \Omega_p + 1} \delta_{\rho_n, \rho'_n} \delta_{\Omega_n, \Omega'_n} \\
& \quad \quad + \langle \rho'_n \Omega'_n | j_n^+ | \rho_n \Omega_n \rangle \delta_{\Omega'_n, \Omega_n + 1} \delta_{\rho_p, \rho'_p} \delta_{\Omega_p, \Omega'_p}) \\
& \quad + \delta_{\sigma} - \delta_{\sigma'} + (\langle \rho'_p \Omega'_p | j_p^+ | \rho_p - \Omega_p \rangle \delta_{\Omega_p, 1/2} \delta_{\Omega'_p, 1/2} \delta_{\rho_n, \rho'_n} \delta_{\Omega_n, \Omega'_n} \\
& \quad \quad + \langle \rho'_n \Omega'_n | j_n^+ | \rho_n - \Omega_n \rangle \delta_{\Omega'_n, 1/2} \delta_{\Omega_n, 1/2} \delta_{\rho_p, \rho'_p} \delta_{\Omega_p, \Omega'_p}) \\
& \quad + \delta_{\sigma} - \delta_{\sigma'} - (\langle \rho'_p \Omega'_p | j_p^+ | \rho_p \Omega_p \rangle \delta_{\Omega'_p, \Omega_p + 1} \delta_{\rho_n, \rho'_n} \delta_{\Omega_n, \Omega'_n} \\
& \quad \quad + \langle \rho'_n \Omega'_n | j_n^+ | \rho_n \Omega_n \rangle \delta_{\Omega'_n, \Omega_n + 1} \delta_{\rho_p, \rho'_p} \delta_{\Omega_p, \Omega'_p})] \delta_{K \neq 0} \\
& \quad + \delta_{K0} \sqrt{I(I+1)} \frac{1}{2} [\delta_{\sigma} - \delta_{\sigma'} + (\langle \rho'_n \Omega'_n | j_n^+ | \rho_n - \Omega \rangle \delta_{\Omega, 1/2} \delta_{\Omega_n, 1/2} \delta_{\Omega \Omega'_p} \delta_{\rho_p \rho'_p} \\
& \quad \quad + (-1)^{I+1} \langle \rho'_p \Omega'_p | j_p^+ | \rho_p - \Omega \rangle \delta_{\Omega, 1/2} \delta_{\Omega'_p, 1/2} \delta_{\Omega \Omega'_n} \delta_{\rho_n \rho'_n}) \\
& \quad \quad + \delta_{\sigma} - \delta_{\sigma'} - (\langle \rho'_p \Omega'_p | j_p^+ | \rho_p \Omega \rangle \delta_{\Omega'_p, \Omega + 1} \delta_{\rho_n, \rho'_n} \delta_{\Omega'_n, \Omega} \\
& \quad \quad + (-1)^{(I+1)} \langle \rho'_n \Omega'_n | j_n^+ | \rho_n \Omega \rangle \delta_{\Omega'_n, \Omega + 1} \delta_{\rho'_p, \rho_p} \delta_{\Omega'_p, \Omega})] \} \\
& + \delta_{K, K'+1} \left[- \frac{\hbar^2}{2\mathcal{J}} \right] \{ [(I-K')(I+K'+1)]^{1/2} \\
& \quad \times [\delta_{\sigma} + \delta_{\sigma'} + (\langle \rho_p \Omega_p | j_p^+ | \rho'_p \Omega'_p \rangle \delta_{\Omega_p, \Omega'_p + 1} \delta_{\rho_n, \rho'_n} \delta_{\Omega_n, \Omega'_n} \\
& \quad \quad + \langle \rho_n \Omega_n | j_n^+ | \rho'_n \Omega'_n \rangle \delta_{\Omega_n, \Omega'_n + 1} \delta_{\rho_p, \rho'_p} \delta_{\Omega_p, \Omega'_p}) \\
& \quad + \delta_{\sigma'} - \delta_{\sigma} + (\langle \rho_p \Omega_p | j_p^+ | \rho'_p - \Omega'_p \rangle \delta_{\Omega_p, 1/2} \delta_{\Omega'_p, 1/2} \delta_{\rho_n, \rho'_n} \delta_{\Omega_n, \Omega'_n} \\
& \quad \quad + \langle \rho_n \Omega_n | j_n^+ | \rho'_n - \Omega'_n \rangle \delta'_{\Omega_n, 1/2} \delta_{\Omega_n, 1/2} \delta_{\rho_p, \rho'_p} \delta_{\Omega_p, \Omega'_p}) \\
& \quad + \delta_{\sigma} - \delta_{\sigma'} - (\langle \rho_p \Omega_p | j_p^+ | \rho'_p \Omega'_p \rangle \delta_{\Omega_p, \Omega'_p + 1} \delta_{\rho_n, \rho'_n} \delta_{\Omega_n, \Omega'_n} \\
& \quad \quad + \langle \rho_n \Omega_n | j_n^+ | \rho'_n \Omega'_n \rangle \delta_{\Omega_n, \Omega'_n + 1} \delta_{\rho_p, \rho'_p} \delta_{\Omega_p, \Omega'_p})] \delta_{K' \neq 0}
\end{aligned}$$

$$\begin{aligned}
& + \delta_{K'0} \sqrt{I(I+1)} \frac{1}{2} [\delta_{\sigma+\delta_{\sigma'}} - (\langle \rho_n \Omega_n | j_n^+ | \rho'_n - \Omega \rangle \delta_{\Omega_n, 1/2} \delta_{\Omega', 1/2} \delta_{\Omega_p \Omega'} \delta_{\rho_p \rho'_p} \\
& \quad + (-1)^{I+1} \langle \rho_p \Omega_p | j_p^+ | \rho'_p - \Omega' \rangle \delta_{\Omega_p, 1/2} \delta_{\Omega', 1/2} \delta_{\Omega_n \Omega'} \delta_{\rho_n \rho'_n}) \\
& \quad + \delta_{\sigma-\delta_{\sigma'}} - (\langle \rho_p \Omega_p | j_p^+ | \rho'_p \Omega' \rangle \delta_{\Omega_p, \Omega'+1} \delta_{\rho_n \rho'_n} \delta_{\Omega_n \Omega'} \\
& \quad + (-1)^{I+1} \langle \rho_n \Omega_n | j_n^+ | \rho'_n \Omega' \rangle \delta_{\Omega_n, \Omega'+1} \delta_{\rho_p \rho'_p} \delta_{\Omega_p \Omega'})] \}. \quad (10)
\end{aligned}$$

Diagonalization of the total Hamiltonian matrix [see Eq. (10)] for each value of the angular momentum I gives us the energies $E_{\text{theor}}(I, \alpha\sigma)$ for all the bands built on the two-quasi-particle configuration $|K\alpha\sigma\rangle$ present in the basis set of eigenfunctions. The total wave functions of these bands are thus linear combinations of (5).

In our approach we have neglected the H_{vib} in Eq. (2). This term represents the long-range residual interaction responsible for vibrations of the core and for coupling between the odd particles and the phonons of the core (polarization effects), see, e.g., Refs. 9–11. Since we are interested only in the low-lying two-quasi-particle states (and the rotational bands built on them) which lie below the collective vibrational excitation of odd-odd nuclei, we expect the coupling of these two-quasi-particle states with vibrational phonons to be small. Small admixtures of phonon components in the two-quasi-particle wave functions can at most lead to minor renormalization of the intrinsic matrix elements of the $j_{n,p}^{\pm}$. A similar situation is found in the particle plus rotor model of odd- A nuclei, where it has been shown that the attenuation of the matrix elements $j_{n,p}^{\pm}$ can be explained by the inclusion of phonon components in the intrinsic wave functions.¹² We believe that a similar situation exists in odd-odd nuclei.

B. The single-particle Hamiltonian

For H_{av} , we use the Nilsson model single-particle Hamiltonian with its standard parametrization for the rare-earth and actinide regions.¹³ The pairing term H_{pair} appears in Eq. (7)–(9) only through the quasiparticle energies ϵ_p and the renormalization of matrix elements of the operators j^{\pm} and V_{np} . It has been shown that the pairing correlations do not contribute to either the G-M splittings or the Newby shifts.⁶ Moreover, as discussed below, since we treat the band energies $E_{\alpha\sigma}$, Eq. (7), the Newby term, Eq. (8), and sometimes the intrinsic matrix elements $\langle \rho' \Omega' | j^+ | \rho \Omega \rangle$ as free parameters, the inclusion of H_{pair} in an exclusive manner is not necessary in our approach.

C. The fitting procedure and selection of parameters

In order to perform a Coriolis-coupling calculation in as complete a fashion as is practical, it is often necessary to consider the mixing of several bands representing the various two-quasi-particle states that are interacting strongly. Since such calculations can involve a large number of parameters, it is most appropriate to select nuclei where many bands have been characterized experimentally. Even then, it is often necessary to estimate the

energies of certain unidentified bands, e.g., the crucial $K=0$ bands whose odd-even staggering can be transmitted to the higher K bands through Coriolis coupling. Therefore, we obtained estimates for the excitation energies of unidentified bands by use of a simple, semiempirical formulation^{1,14,37,40} that employs the known properties (excitation energy and rotational parameter) of given quasiparticle states in neighboring odd- A nuclei. For unidentified bands in odd-odd nuclei, we assumed a constant value $\hbar^2/2\mathcal{J}=13$ keV. The calculations are performed by fitting all of the experimentally known levels in the rotational bands in question. Variable parameters include the band energies and rotational parameters for the experimental levels. The $\langle j^+ \rangle$ matrix elements were calculated using Nilsson wave functions.¹³ The most essential of the matrix elements were also treated as free parameters and were adjusted in the fitting procedure. Another important class of free parameters were the Newby shifts for the $K=0$ bands included in the calculation. In the case where the Newby shift had not been observed for the nucleus in question but had been detected in other nuclei, the experimental value was inserted. The Newby shift E_N can be determined from the energies of two adjacent levels in a $K=0$ band using the expression

$$\begin{aligned}
E_N = & \frac{1}{2} (-1)^{I+1} [E_K(I) - E_K(I-1)] \\
& + \frac{\hbar^2}{2\mathcal{J}} [(-1)^I I - a_p a_n \delta_{\Omega_n, 1/2} \delta_{\Omega_p, 1/2}], \quad (11)
\end{aligned}$$

where a_p and a_n are decoupling parameters for proton and neutron configurations, respectively.

The optimal values for all of the variable parameters were evaluated by minimizing the χ^2 value

$$\chi^2 = \sum_{I, \alpha\sigma} \left[\frac{E_{\text{theor}}(I, \alpha\sigma) - E_{\text{expt}}(I, \alpha\sigma)}{\Delta E_{\text{expt}}(I, \alpha\sigma)} \right]^2, \quad (12)$$

where $\Delta E_{\text{expt}}(I, \alpha\sigma)$ are the experimental errors of the corresponding energy level. We used the MINUIT code¹⁵ to solve this least squares fit problem.

IV. RESULTS AND DISCUSSION

We have carried out Coriolis-coupling calculations for four nuclei: ¹⁶⁸Tm, ¹⁷⁶Lu, ¹⁸²Ta, and ¹⁸²Re. The first three were chosen because there are a large amount of experimental data available for each of them. The nucleus ¹⁸²Re was chosen because a $K=2^+$ and a $K=4^-$ band in this nucleus exhibit significant amounts of staggering which is somewhat unusual for bands with $K > 1$.

Generally, we have succeeded in making precise fits to the levels of rotational bands in these nuclei, even when

the bands exhibit significant staggering. For $K=1$ bands, the magnitude of the observed staggering is a function of the following factors: (1) the Nilsson orbitals occupied by the unpaired nucleons and, hence, the magnitudes of the $\langle j^+ \rangle$ matrix elements connecting $K=0$ and $K=1$ bands; (2) the magnitude of the Newby shift in an interacting $K=0$ band which is also determined by the Nilsson orbitals of the unpaired nucleons; (3) the energy difference between interacting levels; and (4) the number of $K=0$ bands interacting with the $K=1$ band in question. For bands with $K>1$, the observed staggering has been transmitted via mixing with bands where $K=0$ and $K=1$. Thus, staggering in the higher K bands is most likely to be found among orbitals that couple strongly via Coriolis mixing, namely those with high j values such as the configurations arising from the $h_{11/2}$, $i_{13/2}$, and $j_{15/2}$ spherical orbitals. We also find that terms of the particle-particle-coupling type can be important in some cases and may lead to significant admixtures in the wave functions. Since the effects of rotation-particle coupling

and particle-particle coupling are explicitly included in our calculations, we believe the parameters obtained in the level fitting, e.g., the G-M splitting energies and Newby shifts, will be more meaningful. In the following paragraphs, we will discuss those cases where we derive values for the Newby shift that are different from what one might deduce directly from the experimental level energies.

A. ^{176}Lu

In total, 56 rotational bands were included in the Coriolis-mixing calculations for ^{176}Lu . Of these, 16 were experimentally determined. The calculated parameters (band energy, rotational parameter, and Newby shift) derived from the level fitting are given in Table I for the experimentally known bands and for certain $K=0$ bands whose energies were estimated. Also listed in Table I are values for $\langle j^+ \rangle$ matrix elements derived from the level-fitting calculations and their theoretical counterparts.

For ^{176}Lu , a total of 25 experimental levels in 7

TABLE I. Theoretically calculated bandhead energies for all the known bands and all the interacting $K=0$ bands in ^{176}Lu are compared with the experimental data. Also given are the parameter values E_α , $\hbar^2/2\mathcal{J}$, the Newby shift E_N , and those values of $\langle j^+ \rangle$ which were adjusted. The values in the parentheses are from the experimental data (for E_N) in this or other nuclei and from the Nilsson model (for $\langle j^+ \rangle$). The empirical values of the Newby shifts are taken from Ref. 16).

Configuration		$K\pi$	I	E_{expt} (keV)	E_{calc} (keV)	E_α (keV)	$\frac{\hbar^2}{2\mathcal{J}}$	E_N (keV)
Proton	Neutron							
$\frac{7}{2}[404]$	$\frac{7}{2}[514]$	7-	7	0.0	0.0	-73.4	13.20	
$\frac{7}{2}[404]$	$\frac{7}{2}[514]$	0-	0	240.5	240.7	173.0	11.27	-68.9(-69)
$\frac{7}{2}[404]$	$\frac{9}{2}[624]$	1+	1	198.0	198.4	188.0	11.02	
$\frac{7}{2}[404]$	$\frac{9}{2}[624]$	8+	8	404.0	404.1	334.0	12.0	
$\frac{7}{2}[404]$	$\frac{1}{2}[510]$	3-	3	662.0	662.0	626.0	13.0	
$\frac{7}{2}[404]$	$\frac{5}{2}[512]$	1-	1	641.4	641.6	629.3	12.66	
$\frac{5}{2}[402]$	$\frac{7}{2}[514]$	1-	1	390.2	390.4	379.0	12.03	
$\frac{5}{2}[402]$	$\frac{7}{2}[514]$	6-	6	563.9	563.9	496.8	16.21	
$\frac{1}{2}[541]$	$\frac{7}{2}[514]$	4+	4	639.0	638.8	682.0	13.0	
$\frac{9}{2}[514]$	$\frac{7}{2}[514]$	1+	1	342.5	342.5	331.9	11.85	
$\frac{9}{2}[514]$	$\frac{7}{2}[514]$	8+	8	485.7	486.5	432.0	15.29	
$\frac{1}{2}[411]$	$\frac{7}{2}[514]$	4-	4	727.0	726.8	685.0	11.75	
$\frac{1}{2}[411]$	$\frac{7}{2}[514]$	3-	3	838.0	838.0	805.0	11.0	
$\frac{3}{2}[411]$	$\frac{7}{2}[514]$	5-	5	1390.7	1392.3	1341.2	9.70	
$\frac{7}{2}[523]$	$\frac{7}{2}[514]$	0+	0	1057.0	1054.7	1210.6	11.18	155.9(154)
$\frac{7}{2}[523]$	$\frac{7}{2}[514]$	7+	7	1273.0	1277.6	1295.5	12.71	
$\frac{5}{2}[402]$	$\frac{5}{2}[512]$	0-	0		758.9	800.0	12.0	38.0(-28)
$\frac{7}{2}[404]$	$\frac{7}{2}[633]$	0+	0		337.8	464.5	9.61	126.7(42-75)
$\frac{5}{2}[402]$	$\frac{5}{2}[523]$	0-	0		820.7	900.0	12.14	80.0
$\frac{7}{2}[404]$	$\frac{7}{2}[503]$	0-	0		1133.5	1100.0	13.0	-30.0(-26)
$\langle \frac{7}{2}[404] \frac{5}{2}[402] \rangle_p = 1.00(0.47)$				$\langle \frac{7}{2}[514] \frac{5}{2}[512] \rangle_n = 1.20(1.16)$				
$\langle \frac{7}{2}[523] \frac{5}{2}[532] \rangle_p = 4.96(5.05)$				$\langle \frac{7}{2}[514] \frac{5}{2}[523] \rangle_n = -1.82(3.63)$				
$\langle \frac{9}{2}[514] \frac{7}{2}[523] \rangle_p = 4.45(4.39)$				$\langle \frac{9}{2}[624] \frac{7}{2}[633] \rangle_n = 2.19(5.57)$				
$\langle \frac{11}{2}[505] \frac{9}{2}[514] \rangle_p = 0.80(3.31)$				$\langle \frac{11}{2}[615] \frac{9}{2}[624] \rangle_n = 2.88(4.82)$				

positive-parity rotational bands were fitted in the calculations. Of these, the most important to the subject at hand are 18 levels that are distributed evenly among a 0^+ band at 1057 keV and two 1^+ bands at 198 and 342 keV. The assigned configurations for these bands are the following: $0^+ \{ \frac{7}{2}[523]_p - \frac{7}{2}[514]_n \}$, the lower $1^+ \{ \frac{7}{2}[404]_p - \frac{9}{2}[624]_n \}$, and the higher $1^+ \{ \frac{9}{2}[514]_p - \frac{7}{2}[514]_n \}$. Three additional bands with estimated excitation energies were included in the calculation: a $0^+ \{ \frac{7}{2}[404]_p - \frac{7}{2}[633]_n \}$ band at 465 keV, a $2^+ \{ \frac{9}{2}[514]_p - \frac{5}{2}[523]_n \}$ band at 1700 keV, and a $2^+ \{ \frac{7}{2}[404]_p - \frac{11}{2}[615]_n \}$ band at 2000 keV. Thus, two sets of noninteracting bands with $K=0, 1$, and 2 were identified and calculated separately, one including those configurations with a common proton orbital, $\frac{7}{2}[404]_p$, and the other with a common neutron orbital, $\frac{7}{2}[514]_n$. For the purposes of the calculation, these sets were considered to be reasonably self-contained in the sense that no other rotational bands were expected to occur at excitation energies below 2000 keV that would interact strongly with the members of the set.

The energies for 17 of the experimental levels were reproduced well in the calculation, particularly for those levels in the two 1^+ bands where root-mean-squared (rms) deviations were 0.25–0.30 keV for each band. The levels in the 0^+ band were fit with somewhat less precision. The rms deviation for the band was 1.7 keV; however, the experimental energies are also less precise than for the 1^+ bands, e.g., $\pm(1-2)$ keV as compared with $<\pm 0.1$ keV for the 1^+ bands. A poor fit was made to the 5^+ level of the $K=0$ band where the deviation was -16.9 keV (experimental energy = 1730 keV); this result was not included in the calculated deviation for the band. The

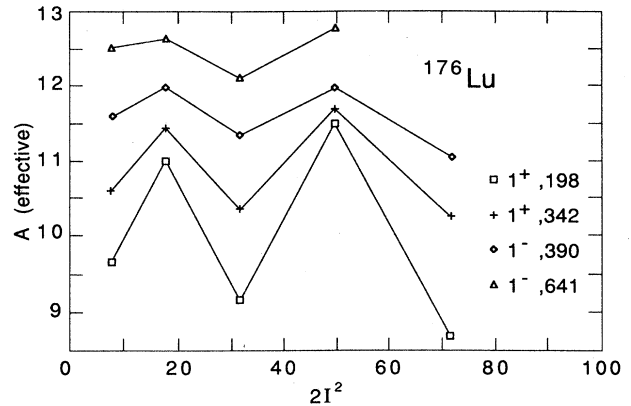


FIG. 4. The staggering plots of four $K=1$ bands in ^{176}Lu are plotted together to show the variation in the magnitude of staggering. See the text for a full discussion.

quality of the fit to experiment can be seen in Fig. 3 where level spacings are plotted as a function of I^2 for the $K=1$ bands of ^{176}Lu and other nuclei. Of course, the levels are fitted in such a way that the calculated values are overdetermined. In this problem, there were 13 parameters that were allowed to vary; these comprised three bandhead energies, four rotational parameters, two Newby shifts, and four $\langle j^+ \rangle$ matrix elements. It should be noted that certain of the $\langle j^+ \rangle$ matrix elements also were used in the fitting of negative parity levels in ^{176}Lu . To the extent that this occurred, the calculation described here is more overdetermined than indicated. Although the quality of the fit obtained here is quite good and one is able to extract values for bandhead energies

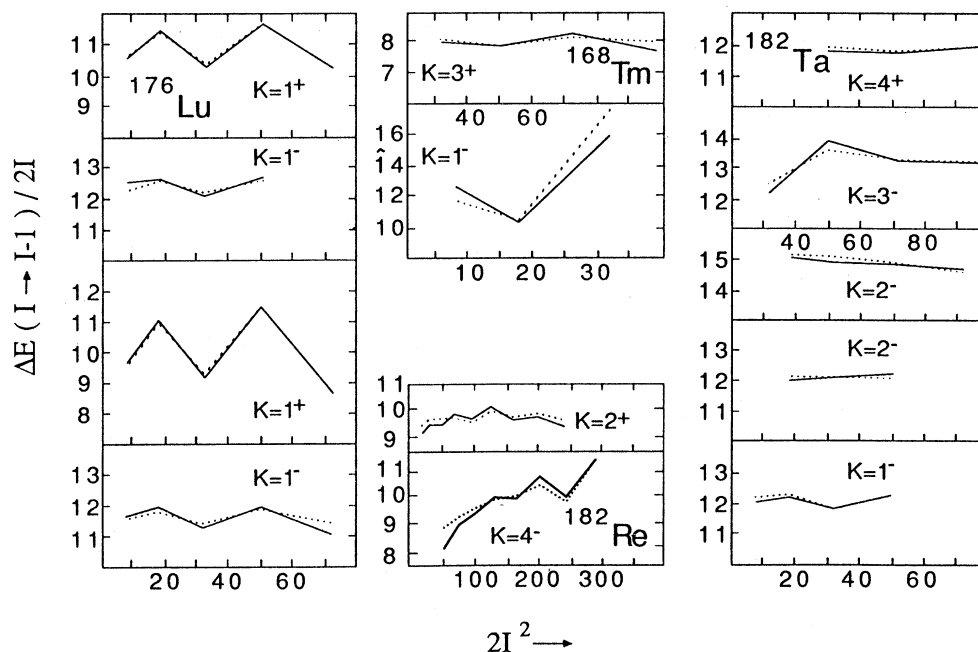


FIG. 3. Results of our calculations (dashed lines) are shown in comparison to the experimental data (solid lines) for the four odd-odd nuclei, ^{168}Tm , ^{176}Lu , ^{182}Ta , and ^{182}Re .

and rotational parameters that have been corrected for the effects of Coriolis mixing, of greater significance, perhaps, are the values of the Newby shifts and $\langle j^+ \rangle$ matrix elements derived from the calculation (see Table I). The Newby shift of the lower-lying 0^+ band, although not known experimentally in ^{176}Lu , was calculated at +127 keV, a value considerably larger than found for this band in other odd-odd nuclei. Of the four $\langle j^+ \rangle$ matrix elements, three had fitted values that were in the range 40–60% of theoretical; the fourth was fitted at essentially 100% of theoretical.

A comparable total number of negative-parity levels, 27, were fitted in calculations for ^{176}Lu . Of these, the levels of most interest to this discussion are the 17 levels distributed among a 0^- band at 126.5 keV and two 1^- bands at 390 and 641 keV. The assigned configurations for these bands are the following: $0^- \{ \frac{7}{2}[404]_p - \frac{7}{2}[514]_n \}$, the lower $1^- \{ \frac{5}{2}[402]_p - \frac{7}{2}[514]_n \}$, and the higher $1^- \{ \frac{7}{2}[404]_p - \frac{5}{2}[512]_n \}$. Three additional bands with estimated excitation energies were included in this calculation: a $0^- \{ \frac{5}{2}[402]_p - \frac{5}{2}[512]_n \}$ band at 800 keV, a $0^- \{ \frac{5}{2}[402]_p - \frac{5}{2}[523]_n \}$ band at 900 keV, and a $0^- \{ \frac{7}{2}[404]_p - \frac{7}{2}[503]_n \}$ band at 1100 keV. The calculations were made allowing all first-order, $\Delta K=1$, Coriolis interactions to occur between these $K=0$ and 1 negative-parity bands.

The energies of 16 of the experimental levels were reproduced fairly well in the calculation; rms deviations were in the range 0.5–0.8 keV for each band. An exception was the 6^- level of the higher 1^- band where the deviation was +4.4 keV (experimental energy=851.8 keV). This result was not included in the calculated deviation for the band. The calculated parameters in this problem were overdetermined; there were 13 variable parameters. One of the $\langle j^+ \rangle$ matrix elements was fitted at 50% of theoretical, while several others were either fitted or assumed to be 100% of theoretical (see Table I). The observed staggering in the two $K=1$ bands is consistent with mixing with $K=0$ bands whose Newby terms are positive. Thus, mixing with the two positively shifted $K=0$ bands at 760 and 820 keV dominates in this problem. For the $K=0$ band, we calculate a Newby shift $E_N = +38$ keV whereas this configuration is thought to

exhibit a negative Newby shift, $E_N = -28$ keV, based upon experimental data for the levels in ^{174}Lu . The interpretation of the experimental data is uncertain enough that the data are considered to provide only tentative evidence for the sign and value of this Newby shift.

The four $K=1$ bands in ^{176}Lu are plotted together in Fig. 4 for comparison. Remarkably, all four bands show odd-even staggering with the same phase, arising from mixing with positively shifted $K=0$ bands. The two positive-parity bands exhibit the greatest magnitude of staggering and also have lower values for their effective rotational parameters. The behavior of these bands can be understood in terms of their strong interactions with higher-lying 0^+ bands, for the band at 198 keV through Coriolis mixing of $[i_{13/2}]_p$ states. As we have already discussed, the situation for the negative-parity $K=1$ bands is more complicated in that there exist several bands with both positive and negative Newby shifts that mix with the bands shown in Fig. 4.

While so far the emphasis in this paper has been on Coriolis mixing of bands with $\Delta K=1$, we find that other types of band mixing arising from the particle-particle-coupling (ppc) term can be important in some cases. This is illustrated by examining the wave functions of levels in the $K=5$, $\{ \frac{3}{2}[411]_p + \frac{7}{2}[514]_n \}$ band at 1391 keV in ^{176}Lu (Table II). A $K=4$, $\{ \frac{5}{2}[402]_p + \frac{3}{2}[512]_n \}$ band mixes strongly in the wave functions; yet, it can only be coupled indirectly to the $K=5$ band by way of ppc interactions, as shown in the coupling diagram of Fig. 5. Also, it is interesting to see significant coupling of a component where $\Delta K=2$, the $K=3$, $\{ \frac{7}{2}[404]_p + \frac{1}{2}[521]_n \}$ configuration.

B. ^{168}Tm

Although a large number of rotational bands have been identified experimentally in ^{168}Tm , the experimental data for this nuclide are somewhat deficient in that no information exists on the gamma-ray transitions between levels. All of the data so far were derived from particle spectroscopy with single-nucleon transfer reactions. Thus, the experimental level energies have uncertainties of 1–3 keV and the spin and parity assignments are untested in terms of the experimentally determined transi-

TABLE II. The admixture of wave functions for the 1391-keV band in ^{176}Lu .

	Proton	Neutron	K	$I=5$	$I=6$	$I=7$	$I=8$	$I=9$
1	$\frac{3}{2}[411]$	$\frac{7}{2}[514]$	5	0.7411	0.9430	0.8593	0.8709	0.8033
2	$\frac{5}{2}[402]$	$\frac{7}{2}[514]$	6		-0.1247	-0.1928	-0.2809	-0.3676
3	$\frac{5}{2}[402]$	$\frac{5}{2}[523]$	5	0.0046	-0.0956	-0.1509	-0.1482	-0.1833
4	$\frac{5}{2}[402]$	$\frac{5}{2}[512]$	5	0.0568	0.0983	0.1252	0.1797	0.2415
5	$\frac{7}{2}[404]$	$\frac{3}{2}[512]$	5	-0.0503	-0.0391	-0.1096	0.0066	-0.0070
6	$\frac{5}{2}[402]$	$\frac{3}{2}[512]$	4	0.5758	0.2323	0.0787	0.2685	0.2842
7	$\frac{5}{2}[402]$	$\frac{1}{2}[510]$	3	0.0516	0.0353	-0.0221	0.1054	0.1230
8	$\frac{7}{2}[404]$	$\frac{1}{2}[510]$	3	-0.0166	-0.276	-0.1672	0.0606	0.0339
9	$\frac{7}{2}[404]$	$\frac{1}{2}[521]$	3	-0.3191	-0.1098	-0.1816	-0.0269	-0.0547

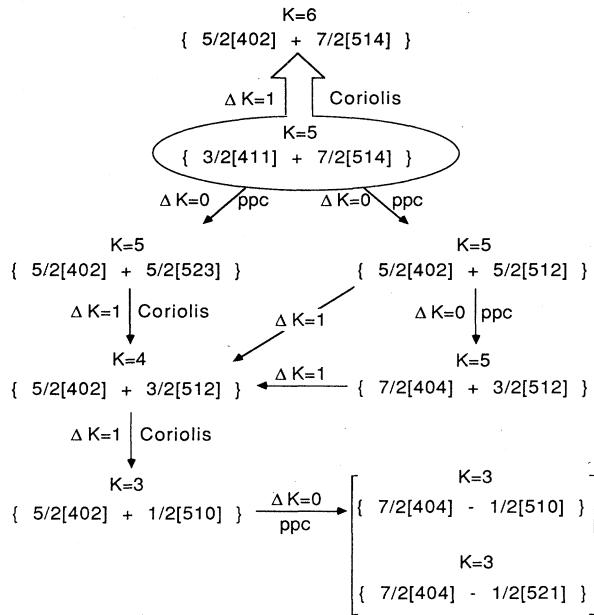


FIG. 5. The complex structure of the 1391 keV $K=5$ band wave function is explained by the many couplings shown in this figure. See the text for a full discussion.

tion multiplicities. In total, 56 bands were included in our Coriolis-mixing calculations for ^{168}Tm . The experimental data are comprised of 59 levels assigned to 24 rotational bands. In fitting these levels, the number of variable parameters was nearly equal to the number of levels; the problem was barely overdetermined. The fitted values for the variable parameters are listed in Table III. The rotational spacings of the two lowest-lying bands, those with $K=3^+$ and 1^- , are fitted adequately in the calculation, as can be seen in Fig. 3. In our calculation, a significantly different value for the Newby shift in the $0^- \{ \frac{1}{2}[411]_p - \frac{1}{2}[521]_n \}$ band was found as compared with a value of 26.9 keV that can be extracted directly from the experimental level energies. For this band, it appears from the calculation that the most likely spin assignments for the levels at 226 and 238 keV are $I=2$ and $I=1$, respectively, rather than the reverse. There are several negative-parity bands whose levels lie in the energy range 600–1000 keV and mix together strongly. Thus, a precise calculation of the levels in a $K=1^-$ band assigned at 611 keV has not been attempted.

C. ^{182}Ta

In total, 60 bands were included in the Coriolis-mixing calculation for ^{182}Ta . The experimental data are comprised of 55 levels assigned to 18 rotational bands. The different variable parameters totaled 50; all of these are listed in Table IV. Among the negative-parity bands, the rotational spacings were fit well, as shown in Fig. 3. For the $K=1$ band, the rms deviation is 0.3 keV; for the $K=3$ band, the rms deviation is 0.7 keV. The staggering observed in the $1^- \{ \frac{5}{2}[402]_p - \frac{3}{2}[512]_n \}$ band is accurately

reproduced, assuming it results from the influence of a $0^- \{ \frac{3}{2}[411]_p - \frac{3}{2}[512]_n \}$ band calculated to occur at 617 keV. The staggering or perturbation observed in the $3^- \{ \frac{7}{2}[404]_p - \frac{1}{2}[510]_n \}$ band does not arise so much from any higher-order coupling to a $K=0$ band, but rather from the coupling with its G-M partner, the $4^- \{ \frac{7}{2}[404]_p + \frac{1}{2}[510]_n \}$ band. The Coriolis interaction between these bands produces perturbations, particularly in the $I=3,4$ and $I=4,5$ level spacings, while levels with greater angular momentum show regular, rather linear behavior when plotted as in Fig. 3. In the calculation of positive-parity bands, the calculated Newby shift for the unobserved $0^+ \{ \frac{7}{2}[404]_p - \frac{7}{2}[633]_n \}$ band is +130 keV, a value similar to that calculated for this same band in the ^{176}Lu problem and also appreciably larger than found experimentally in other nuclei.

D. ^{182}Re

Slaughter *et al.*² have identified four bands in ^{182}Re and have made Nilsson assignments on the basis of many experimental and theoretical arguments. These bands comprise two K^- bands ($K=2^+$ and $K=4^-$) and two K^+ bands ($K=7^+$ and 9^-). The former both display large odd-even staggering; the latter do not. The $K=7^+$ (ground state) and $K=2^+$ bands are assigned to the G-M doublet, $\{ \frac{5}{2}[402]_p \pm \frac{9}{2}[624]_n \}$. The $K=9^-$ band occurs at 443.6 keV; the excitation energies of the K^- bands have not been determined. Based on a calculated G-M matrix element,⁶ the 2^+ band is assumed to occur at approximately 100 keV; it is known experimentally that the 4^- band lies 461.3 keV above the 2^+ band.

In total, 30 rotational bands were included in the Coriolis-mixing calculations for ^{182}Re . There have been 24 levels identified experimentally and assigned to the four known bands. The levels of both positive-parity bands were fitted in our calculation, but it is the nine experimental levels of the 2^+ band that are of most concern. These levels were fitted in a calculation where six quantities were varied freely (three band energies, two rotational parameters, and one Newby shift), while an additional three $\langle j^+ \rangle$ matrix elements were permitted to vary, but in concert with the calculations made for the three other experimental bands. Values of the variable quantities are listed in Table V. The rotational spacings in this band were fit well, as shown in Fig. 3. The rms deviation for the levels in the 2^+ band is 1.4 keV. The observed staggering is the result of mixing with the $1^+ \{ \frac{5}{2}[402]_p \pm \frac{7}{2}[633]_n \}$ and $0^+ \{ \frac{5}{2}[402]_p \pm \frac{5}{2}[624]_n \}$ bands. For the latter band, we calculate a Newby shift of -25 keV; this band has not been identified experimentally in ^{182}Re or other nuclei. It is of interest to note that our calculated result is in agreement with an empirical rule for the sign of Newby shifts in $K=0$ rotational bands from pure j shells proposed by Frisk.¹⁶

The 15 levels of the negative-parity bands were also fitted in our calculations. Of these, the nine levels in the $4^- \{ \frac{1}{2}[541]_p - \frac{9}{2}[624]_n \}$ band were of greatest interest. These were fit in a calculation that included 12 rotational bands, 6 each in the $K^+ \{ \frac{1}{2}[541]_p + [i_{13/2}]_n \}$ series and the $K^- \{ \frac{1}{2}[541]_p - [i_{13/2}]_n \}$ series. Three quantities (two

band energies and one rotational parameter) were treated as variables, while various values were inserted in the calculation for the Newby shift in the $0^- \{ \frac{1}{2}[541]_p - \frac{1}{2}[660]_n \}$ band. Seven different $\langle j^+ \rangle$ matrix elements were also varied, but five of these were additionally constrained in the calculations for the positive-parity bands. Although the fit to the level energies of this 4^- band is quite ordinary (the rms deviation is 5.2 keV),

the odd-even staggering is faithfully reproduced (Fig. 3). Since this phenomenon has seldom been observed in rotational bands with K quantum numbers as large as 4, it is of considerable interest to understand the origin of the observed odd-even perturbations.

The experimentally observed 4^- band is thought to be the lowest-lying member of the K^- series, $\{ \frac{1}{2}[541]_p - [i_{13/2}]_n \}$. Among the neutron orbitals, the

TABLE III. Theoretically calculated bandhead energies for all the known bands and all the interacting $K=0$ bands in ^{168}Tm are compared with the experimental data. Also given are the parameter values E_α , $\hbar^2/2\mathcal{J}$, the Newby shift E_N , and those values of $\langle j^+ \rangle$ which were adjusted. The values in the parentheses are from the experimental data (for E_N) in this or other nuclei and from the Nilsson model (for $\langle j^+ \rangle$). The empirical values of the Newby shifts are taken from Ref. 16.

Configuration		$K\pi$	I	E_{expt} (keV)	E_{calc} (keV)	E_α (keV)	$\frac{\hbar^2}{2\mathcal{J}}$	E_N (keV)
Proton	Neutron							
$\frac{1}{2}[411]$	$\frac{7}{2}[633]$	3+	3	0.0	0.0	1.9	12.68	
$\frac{1}{2}[411]$	$\frac{7}{2}[633]$	4+	4	148.0	148.2	145.6	10.05	
$\frac{1}{2}[411]$	$\frac{1}{2}[521]$	1-	1	3.0	2.5	-6.5	10.67	
$\frac{1}{2}[411]$	$\frac{1}{2}[521]$	0-	0	164.0	159.6	187.9	10.96	43.5(26)
$\frac{1}{2}[411]$	$\frac{5}{2}[512]$	2-	3	322	319.5	305.1	7.80	
$\frac{1}{2}[411]$	$\frac{3}{2}[512]$	3-	4	389	394.4	324.2	10.42	
$\frac{1}{2}[411]$	$\frac{5}{2}[523]$	3-	3	857	863.4	831.0	11.0	
$\frac{1}{2}[411]$	$\frac{3}{2}[523]$	2-	2	899	898.8	876.0	11.0	
$\frac{1}{2}[411]$	$\frac{3}{2}[521]$	1-	1	611	613.1	607.3	11.41	
$\frac{1}{2}[411]$	$\frac{3}{2}[521]$	2-	2	699	695.8	695.9	11.0	
$\frac{1}{2}[411]$	$\frac{1}{2}[510]$	0-	1	789	789.0	765.8	10.05	0.56
$\frac{1}{2}[411]$	$\frac{1}{2}[510]$	1-	2	882	880.4	783.3	12.56	
$\frac{1}{2}[411]$	$\frac{1}{2}[400]$	0+	0	1057	1060.2	1081.1	11.67	22.4(18)
$\frac{1}{2}[411]$	$\frac{1}{2}[400]$	1+	1	1348	1348.0	1337.4	9.0	
$\frac{1}{2}[411]$	$\frac{3}{2}[402]$	2+	2	1116	1116.2	1094.9	11.68	
$\frac{1}{2}[411]$	$\frac{3}{2}[402]$	1+	1	1427	1426.9	1414.0	12.76	
$\frac{1}{2}[541]$	$\frac{7}{2}[633]$	3-	4	200	204.0	244.1	9.06	
$\frac{1}{2}[541]$	$\frac{7}{2}[633]$	4-	4	337	348.4	250.8	12.30	
$\frac{7}{2}[404]$	$\frac{7}{2}[633]$	0+	0	17	16.3	57.0	13.0	40.0(42)
$\frac{7}{2}[404]$	$\frac{7}{2}[633]$	7+	7	312	312.3	275.0	13.0	
$\frac{5}{2}[402]$	$\frac{7}{2}[633]$	6+	6	731	728.2	676.0	13.0	
$\frac{5}{2}[402]$	$\frac{7}{2}[633]$	1+	1	815	815.3	809.3	8.10	
$\frac{1}{2}[530]$	$\frac{7}{2}[633]$	4-	4	1389	1401.2	1321.4	11.40	
$\frac{1}{2}[530]$	$\frac{7}{2}[633]$	3-	3	1439	1451.1	1399.2	7.04	
$\frac{7}{2}[523]$	$\frac{7}{2}[633]$	0-	0		368.0	400.0	13.0	32.0

$$\langle \frac{1}{2}[411] | \frac{1}{2}[411] \rangle_p = 0.72(0.96)$$

$$\langle \frac{1}{2}[541] | \frac{1}{2}[541] \rangle_p = -1.97(-3.78)$$

$$\langle \frac{1}{2}[541] | \frac{1}{2}[530] \rangle_p = -3.21(-2.41)$$

$$\langle \frac{1}{2}[530] | \frac{1}{2}[530] \rangle_p = 0.64(2.56)$$

$$\langle \frac{3}{2}[402] | \frac{3}{2}[411] \rangle_p = 2.64(2.34)$$

$$\langle \frac{1}{2}[521] | \frac{1}{2}[521] \rangle_n = -1.98(-0.84)$$

$$\langle \frac{1}{2}[521] | \frac{1}{2}[510] \rangle_n = 1.68(2.60)$$

$$\langle \frac{1}{2}[510] | \frac{1}{2}[510] \rangle_n = 0.10(-0.01)$$

$$\langle \frac{1}{2}[400] | \frac{1}{2}[400] \rangle_n = -0.19(-0.14)$$

$$\langle \frac{3}{2}[521] | \frac{1}{2}[521] \rangle_n = -0.67(-0.23)$$

$$\langle \frac{3}{2}[521] | \frac{1}{2}[510] \rangle_n = 2.79(1.56)$$

$$\langle \frac{5}{2}[512] | \frac{3}{2}[521] \rangle_n = 3.83(3.73)$$

$$\langle \frac{5}{2}[523] | \frac{3}{2}[521] \rangle_n = 0.40(1.29)$$

$$\langle \frac{7}{2}[633] | \frac{5}{2}[642] \rangle_n = 4.85(6.13)$$

$$\langle \frac{9}{2}[624] | \frac{7}{2}[633] \rangle_n = 1.89(5.63)$$

$$\langle \frac{7}{2}[514] | \frac{5}{2}[512] \rangle_n = 1.30(1.17)$$

$$\langle \frac{7}{2}[514] | \frac{5}{2}[523] \rangle_n = 1.69(3.61)$$

$\frac{9}{2}[624]$ orbital is known to occur lowest, in fact as the ground state, in ^{181}W . Also, it displays in ^{181}W very significant odd-even staggering whose amplitude increases dramatically with increasing angular momentum. In ^{182}Re odd-even staggering is the product of the Newby shift in the $K=0^- \{ \frac{1}{2}[541]_p - \frac{1}{2}[660]_n \}$ band which we estimate to exist at 2000 keV. Since this band has $\Omega_p = \Omega_n = \frac{1}{2}$, the observed shift between the odd- and even-spin members of the band will include contributions both from the usual matrix element that arises from the residual n - p interaction and from a term of the form $(\hbar^2/2\mathcal{J})a_p a_n$. This latter term will be rather large, 217 keV if one adopts the values given in Table V. Since the signs of the a_p and a_n values are the same and if one assumes a nominal value of 100 keV (or less) for the matrix element from the residual interaction, the magnitude of the Newby shift in this band will be largest if the matrix element has a positive sign. An interesting point is that

the phase of the odd-even staggering observed in the 4^- band is opposite to that expected if the elements of the Newby shift are positive.

An even more significant origin for the observed staggering has been found to exist, however. This is the odd-even staggering that occurs in the $K^+ \{ \frac{1}{2}[541]_p + [i_{13/2}]_n \}$ series of rotational bands that also exist in ^{182}Re . The $K=1$ band in this series couples to the $K=0$ band previously discussed through $\Delta K=1$ Coriolis mixing, but it is the nature of the matrix element for this coupling that is of interest. The matrix element takes the form

$$(-\hbar^2/2\mathcal{J})[I(I+1)]^{1/2}[a_p + a_n(-1)^{I+1}].$$

Thus, the *Coriolis mixing* has an odd-even alteration in absolute magnitude of the matrix elements. The K^+ series of bands display an interesting property in that the lower-lying members of the series are rotational bands

TABLE IV. Theoretically calculated bandhead energies for all the known bands and all the interacting $K=0$ bands in ^{182}Ta are compared with the experimental data. Also given are the parameter values E_α , $\hbar^2/2\mathcal{J}$, the Newby shift E_N , and those values of $\langle j^+ \rangle$ which were adjusted. The values in the parentheses are from the experimental data (for E_N) in this or other nuclei and from the Nilsson model (for $\langle j^+ \rangle$). The empirical values of the Newby shifts are taken from Ref. 16.

Configuration		$K\pi$	I	E_{expt} (keV)	E_{calc} (keV)	E_α (keV)	$\frac{\hbar^2}{2\mathcal{J}}$	E_N (keV)
Proton	Neutron							
$\frac{7}{2}[404]$	$\frac{1}{2}[510]$	3-	3	0.0	0.0	-38.1	13.36	
$\frac{7}{2}[404]$	$\frac{1}{2}[510]$	4-	4	114.0	117.8	40.3	17.8	
$\frac{7}{2}[404]$	$\frac{9}{2}[624]$	1+	1	592.9	592.8	584.0	8.76	
$\frac{7}{2}[404]$	$\frac{3}{2}[512]$	5-	5	173.0	173.1	114.5	12.41	
$\frac{7}{2}[404]$	$\frac{3}{2}[512]$	2-	2	270.0	268.9	239.2	15.62	
$\frac{7}{2}[404]$	$\frac{7}{2}[503]$	0-	0	584.0	584.5	558.0	13.5	-26.5(-26)
$\frac{7}{2}[404]$	$\frac{7}{2}[503]$	7-	7	777.0	778.7	684.3	13.74	
$\frac{7}{2}[404]$	$\frac{11}{2}[615]$	2+	2	402.6	402.7	390.5	16.03	
$\frac{7}{2}[404]$	$\frac{7}{2}[514]$	7-	7	1116.2	1118.1	1025.0	13.99	
$\frac{9}{2}[514]$	$\frac{1}{2}[510]$	5+	5	16.5	16.4	-43.0	13.41	
$\frac{9}{2}[514]$	$\frac{1}{2}[510]$	4+	4	150.4	150.0	104.7	12.43	
$\frac{9}{2}[514]$	$\frac{9}{2}[624]$	9-	9	652.6	652.0	535.0	13.0	
$\frac{9}{2}[514]$	$\frac{3}{2}[512]$	3+	3	250.0	250.1	208.9	14.82	
$\frac{9}{2}[514]$	$\frac{3}{2}[512]$	6+	6	397.0	397.9	323.2	13.81	
$\frac{9}{2}[514]$	$\frac{11}{2}[615]$	10-	10	519.8	519.7	477.5	11.84	
$\frac{5}{2}[402]$	$\frac{1}{2}[510]$	3-	3	547.1	546.7	510.2	14.41	
$\frac{5}{2}[402]$	$\frac{1}{2}[510]$	2-	2	647.7	647.2	625.1	12.96	
$\frac{5}{2}[402]$	$\frac{3}{2}[512]$	1-	1	443.6	443.4	432.4	12.78	
$\frac{7}{2}[404]$	$\frac{7}{2}[514]$	0-	0		1269.9	1200.0	13.80	-70.0(-69)
$\frac{7}{2}[404]$	$\frac{7}{2}[633]$	0+	0		420.0	550.0	9.0	130.0(35-56)
$\frac{3}{2}[411]$	$\frac{3}{2}[512]$	0-	0		616.6	627.3	9.86	9.5

$\langle \frac{7}{2}[404] \frac{5}{2}[402] \rangle_p = 0.64(0.48)$	$\langle \frac{3}{2}[512] \frac{1}{2}[510] \rangle_n = -0.33(-0.33)$
$\langle \frac{9}{2}[514] \frac{7}{2}[523] \rangle_p = 2.16(4.40)$	$\langle \frac{3}{2}[501] \frac{1}{2}[510] \rangle_n = -1.65(-1.85)$
$\langle \frac{1}{2}[510] \frac{1}{2}[510] \rangle_n = -0.20(-1.01)$	$\langle \frac{5}{2}[503] \frac{3}{2}[512] \rangle_n = 1.50(1.16)$
$\langle \frac{9}{2}[624] \frac{7}{2}[633] \rangle_n = 0.20(5.54)$	$\langle \frac{11}{2}[615] \frac{9}{2}[624] \rangle_n = 3.11(4.81)$

TABLE V. Theoretically calculated bandhead energies for all the known bands and all the interacting $K=0$ bands in ^{182}Re are compared with the experimental data. Also given are the parameter values E_α , $\hbar^2/2\mathcal{J}$, the Newby shift E_N , and those values of $\langle j^+ \rangle$ which were adjusted. The values in the parentheses are from the experimental data (for E_N) in this or other nuclei and from the Nilsson model (for $\langle j^+ \rangle$). The empirical values of the Newby shifts are taken from Ref. 16.

Configuration		$K\pi$	I	E_{expt} (keV)	E_{calc} (keV)	E_α (keV)	$\frac{\hbar^2}{2\mathcal{J}}$	E_N (keV)
Proton	Neutron							
$\frac{5}{2}[402]$	$\frac{9}{2}[624]$	7+	7	0	0	-74.5	13.9	
$\frac{5}{2}[402]$	$\frac{9}{2}[624]$	2+	2	(100.0)	98.5	84.1	12.6	
$\frac{1}{2}[541]$	$\frac{9}{2}[624]$	9-	9	443.1	443.1	424.2	14.5	
$\frac{1}{2}[541]$	$\frac{9}{2}[624]$	4-	4	(561.3)	553.1	528.3	15.4	
$\frac{1}{2}[541]$	$\frac{9}{2}[624]$	5-	5		857.7	821.6	15.6	
$\frac{5}{2}[402]$	$\frac{5}{2}[642]$	0+	0		1083.5	1031.9	8.5	-25.1
$\frac{1}{2}[541]$	$\frac{1}{2}[660]$	0-	0		2092.5	2000.0	13.5	-50.0
$\langle \frac{5}{2}[402] \frac{3}{2}[411] \rangle_p = 1.40(2.38)$				$\langle \frac{1}{2}[660] \frac{1}{2}[660] \rangle_n = -6.72(-6.72)$				
$\langle \frac{7}{2}[404] \frac{5}{2}[402] \rangle_p = 0.48(0.48)$				$\langle \frac{3}{2}[651] \frac{1}{2}[660] \rangle_n = 5.65(6.65)$				
$\langle \frac{3}{2}[411] \frac{1}{2}[411] \rangle_p = -1.17(-1.17)$				$\langle \frac{5}{2}[642] \frac{3}{2}[651] \rangle_n = 5.34(6.44)$				
$\langle \frac{9}{2}[514] \frac{7}{2}[523] \rangle_p = 3.35(4.40)$				$\langle \frac{7}{2}[633] \frac{5}{2}[642] \rangle_n = 3.54(6.10)$				
$\langle \frac{1}{2}[541] \frac{1}{2}[541] \rangle_p = -2.10(-4.60)$				$\langle \frac{9}{2}[624] \frac{7}{2}[633] \rangle_n = 3.51(5.59)$				

with odd-even staggering of a certain phase and the higher-lying members of the series are rotational bands with odd-even staggering of the *opposite* phase. Finally, then, the low-lying $K=5$ band of the K^+ series interacts with the experimentally seen $K=4$ band of the K^- series (the matrix element here is equal in magnitude to a_p , or 2.1 keV). For ^{182}Re , this interaction is dominant and is responsible for the observed odd-even staggering. A value of +50 keV was assumed for the residual-interaction matrix; the calculation proved to be somewhat insensitive to the value assumed.

V. CONCLUSIONS

We observe an odd-even staggering in most of the K^- bands of odd-odd rare-earth and actinide nuclei. To explain the staggering, which is observed in $K^- = 1, 2, 3,$ and 4 bands, we have done detailed Coriolis-mixing calculations that are nearly complete in the sense that all the important bands with either known or estimated energies were taken into account. Successful reproduction of the odd-even staggering in four nuclei, where calculations were done, implies that the odd-even staggering is indeed a result of Coriolis mixing. An analysis of the results revealed that at least three mechanisms may be responsible for the odd-even staggering. The most important of these is mixing with Newby-shifted $K=0$ bands, which occurs directly in the case of $K=1$ bands and through successive $\Delta K=1$ Coriolis couplings for bands with $K>1$. Some perturbations in level spacings can be seen when there is multiple band mixing with successively increasing values of K . Finally, at much higher angular momenta than considered here, the decoupling of an unpaired nucleon

and bandcrossings can contribute to staggered behavior in rotational bands.

Also, it has become clear from our study that K^- bands are more staggered than K^+ bands because the former can be coupled more directly to Newby-shifted $K=0$ bands. The amount of staggering may be large or small depending on a number of factors such as Nilsson orbitals occupied by the unpaired nucleons, the value of $\langle j^+ \rangle$, and the closeness and the number of interacting $K=0$ bands.

Our calculations reveal the importance of coupling terms other than the Coriolis term, namely those that describe particle-particle coupling in the Hamiltonian. We find that this may lead to an admixture of configurations in the wave functions that are coupled to the main component in the third and the fourth order.

We can also calculate pure values of the Newby shift (E_N) and the G-M splitting energy that are free from the Coriolis-admixture effects. These values in many cases differ significantly from those found directly from the data by using a diagonal expression. We consider these values as more appropriate for comparison with theoretical calculations.

ACKNOWLEDGMENTS

This study was supported by the National Science Foundation under Contract No. PHY-8605032 with Florida State University and the Department of Energy under Contract No. W-7405-ENG-48 with the Lawrence Livermore National Laboratory. One of us (J.K.) acknowledges support from the International Research and Exchange Board, New Jersey during the course of this work.

- *Permanent address: Department of Physics, University of Roorkee, Roorkee-247667, India.
- †Permanent address: Department of Nuclear Physics, Charles University, CS-18000 Prague, Czechoslovakia.
- ¹H. T. Motz, E. T. Journey, O. W. B. Schult, H. R. Koch, U. Gruber, P. B. Maier, H. Baader, G. L. Struble, J. Kern, R. K. Sheline, T. von Egidy, Th. Elze, E. Bieber, and A. Bäcklin, *Phys. Rev.* **155**, 1265 (1967).
- ²M. F. Slaughter, R. A. Warner, T. L. Khoo, W. H. Kelly, and W. C. McHarris, *Phys. Rev. C* **29**, 114 (1984).
- ³A. K. Jain, J. Kvasil, R. K. Sheline, and R. W. Hoff, *Phys. Lett. B* **209**, 19 (1988).
- ⁴J. A. Pinston, S. Andre, D. Barneoud, C. Foin, J. Genevey, and H. Frisk, *Phys. Lett.* **137B**, 47 (1984), and references therein.
- ⁵N. D. Newby, *Phys. Rev.* **125**, 2063 (1962).
- ⁶J. P. Boisson, R. Piepenbring, and W. Ogle, *Phys. Rep.* **26C**, 99 (1976).
- ⁷F. Sterba, L. Nosek, J. Kvasil, and P. Holan (submitted to *Czech. J. Phys.*).
- ⁸D. Elmore and W. P. Alford, *Nucl. Phys.* **A273**, 1 (1976).
- ⁹V. G. Soloviev, *Phys. Lett.* **21**, 320 (1966).
- ¹⁰V. G. Soloviev, *Theory of Complex Nuclei* (Pergamon Press, Oxford, 1976).
- ¹¹L. S. Kisslinger and R. A. Sorensen, *Rev. Mod. Phys.* **35**, 853 (1963).
- ¹²J. Kvasil, I. N. Mikhailov, R. Ch. Safarov, and B. Choriev, *Czech. J. Phys. B* **28**, 843 (1978).
- ¹³S. G. Nilsson, C. F. Tsang, A. Sobiczewski, Z. Szymanski, S. Wycech, C. Gustafson, I.-L. Lamm, P. Möller, and B. Nilsson, *Nucl. Phys.* **A131**, 1 (1969).
- ¹⁴P. C. Sood, R. W. Hoff, and R. K. Sheline, *Phys. Rev. C* **33**, 2163 (1986).
- ¹⁵F. James and M. Ross, *Comput. Phys. Commun.* **10**, 343 (1975).
- ¹⁶H. Frisk, *Z. Phys. A* **330**, 241 (1988).
- ¹⁷*Table of Isotopes*, 7th ed., edited by C. M. Lederer and V. S. Shirley (Wiley, New York, 1978).
- ¹⁸H. Rotter, C. Heiser, K. D. Schilling, W. Andrejtscheff, L. K. Kostov, and M. K. Balodis, *Nucl. Phys.* **A417**, 1 (1984).
- ¹⁹M. K. Balodis, P. T. Prokofjev, N. D. Kramer, L. I. Simonova, K. Schreckenbach, W. F. Davidson, J. A. Pinston, P. Hungerford, H. H. Schmidt, H. J. Scheerer, T. Von Egidy, P. H. M. Van Assche, A. M. J. Spits, R. F. Casten, W. R. Kane, D. D. Warner, and J. Kern, *Nucl. Phys.* **A472**, 445 (1987).
- ²⁰K. D. Schilling, L. Kaubler, W. Andrejtscheff, T. M. Muminov, V. G. Kalinnikov, N. Z. Marupov, F. R. May, and W. Seidel, *Nucl. Phys.* **A299**, 189 (1978).
- ²¹H. D. Jones and R. K. Sheline, *Nucl. Phys.* **A150**, 497 (1970).
- ²²J. J. Basman and H. Postma, *Nucl. Phys.* **A320**, 260 (1979).
- ²³H. D. Jones and R. K. Sheline, *Ann. Phys. (N.Y.)* **63**, 28 (1971).
- ²⁴J. J. Kolata and J. V. Maher, *Phys. Rev. C* **8**, 285 (1975).
- ²⁵Z. Preibisz, D. G. Burke, and R. A. O'Neil, *Nucl. Phys.* **A201**, 86 (1973).
- ²⁶G. L. Struble, R. G. Lanier, L. G. Mann, R. T. Kouzes, D. Mueller, R. A. Naumann, F. Girschick, I. C. Oelrich, and W. H. Moore, *Phys. Rev. Lett.* **40**, 615 (1978).
- ²⁷J. Kern, A. Bruder, J.-Cl. Dousse, M. Gasser, V. A. Ionescu, R. Lanners, B. Perny, B. Piller, Ch. Rheme, and B. Schaller, *Phys. Lett.* **146B**, 183 (1984).
- ²⁸A. Bruder, J. C. Dousse, S. Drissi, M. Gasser, V. A. Ionescu, J. Kern, B. Perny, M. Rast, and C. Rheme, *Nucl. Phys.* **A467**, 1 (1987).
- ²⁹A. Bruder, S. Drissi, V. A. Ionescu, J. Kern, and J. P. Vorlet, *Nucl. Phys.* **A474**, 518 (1987).
- ³⁰M. K. Balodis, J. J. Tamberg, K. J. Alksnis, P. T. Prokofjev, W. G. Vonach, H. K. Vonach, H. R. Koch, U. Gruber, B. P. K. Maier, and O. W. B. Schult, *Nucl. Phys.* **A194**, 305 (1972).
- ³¹R. A. Dewberry, R. K. Sheline, R. G. Lanier, L. G. Mann, and G. L. Struble, *Phys. Rev. C* **24**, 1628 (1981).
- ³²R. A. Dewberry and R. A. Naumann, *Phys. Rev. C* **28**, 2259 (1983).
- ³³E. Warde, G. J. Costa, D. Magnac, R. Seltz, C. Gerardin, M. Buenerd, Ph. Martin, W. Saathoff, and C. A. Wiedner, *Phys. Rev. C* **27**, 98 (1983).
- ³⁴E. Hagn and G. Eska, *Nucl. Phys.* **A363**, 269 (1981).
- ³⁵E. B. Shera, U. Gruber, B. P. K. Maier, H. R. Koch, O. W. B. Schult, R. G. Lanier, N. Onishi, and R. K. Sheline, *Phys. Rev. C* **6**, 537 (1972).
- ³⁶F. Sterba, P. Holan, J. Kvasil, M. Horakova, and R. K. Sheline, *Czech. J. Phys. B* **29**, 1215 (1979).
- ³⁷R. W. Hoff, *Inst. Phys. Conf. Ser.* **88**, 343 (1988); *J. Phys. G Suppl.* **14**, 343 (1988).
- ³⁸V. A. Ionescu, J. Kern, R. F. Casten, W. R. Kane, I. Ahmad, J. Erskine, A. M. Friedman, and K. Katori, *Nucl. Phys.* **A313**, 283 (1979).
- ³⁹T. Grottdal, L. Guldberg, K. Nybo, and T. F. Thorsteinsen, *Phys. Scr.* **14**, 263 (1976).
- ⁴⁰T. Von Egidy, R. W. Hoff, R. W. Loughheed, D. H. White, H. G. Börner, K. Schreckenbach, D. D. Warner, G. Barreau, and P. Hungerford, *Phys. Rev. C* **29**, 1243 (1984).